

Semi-Decentralized Federated Edge Learning for Fast Convergence on Non-IID Data

Yuchang Sun, Jiawei Shao, Yuyi Mao, and Jun Zhang

Department of Electronic and Information Engineering

The Hong Kong Polytechnic University, Hong Kong

Email: {yuchang.sun, jiawei.shao}@connect.polyu.hk, {yuyi-eie.mao, jun-eie.zhang}@polyu.edu.hk

Abstract—Federated edge learning (FEEL) has emerged as an effective alternative to reduce the large communication latency in Cloud-based machine learning solutions, while preserving data privacy. Unfortunately, the learning performance of FEEL may be compromised due to limited training data in a single edge cluster. In this paper, we investigate a novel framework of FEEL, namely semi-decentralized federated edge learning (SD-FEEL). By allowing model aggregation between different edge clusters, SD-FEEL enjoys the benefit of FEEL in reducing training latency and improves the learning performance by accessing richer training data from multiple edge clusters. A training algorithm for SD-FEEL with three main procedures in each round is presented, including local model updates, intra-cluster and inter-cluster model aggregations, and it is proved to converge on non-independent and identically distributed (non-IID) data. We also characterize the interplay between the network topology of the edge servers and the communication overhead of inter-cluster model aggregation on training performance. Experiment results corroborate our analysis and demonstrate the effectiveness of SD-FEEL in achieving fast convergence. Besides, guidelines on choosing critical hyper-parameters of the training algorithm are also provided.

Index Terms—Federated learning, non-IID data, distributed machine learning, communication efficiency.

I. INTRODUCTION

The recent development of machine learning (ML) technologies has led to major breakthroughs in various domains. Meanwhile, the number of Internet of Things (IoT) devices is growing at a drastic speed, and it is envisaged to reach more than 30 billion IoT devices by 2025 [1]. This results in a huge volume of data generated at the edge of the wireless network, which then support the training of powerful ML models. A traditional approach is to upload these data to a centralized server for model training. However, offloading data raises severe privacy concerns as data collected by IoT devices, e.g., smartphones and healthcare sensors, may contain privacy-sensitive information [2].

To resolve the privacy issues in centralized ML, federated learning (FL) was proposed by Google in 2017 as a privacy-preserving distributed ML paradigm [3]. FL enables IoT devices to collaboratively learn a shared ML model without disclosing their local data. A typical FL system consists of a Cloud-based parameter server (PS) and a number of client nodes which train a deep learning (DL) model via multiple global iterations. In each global iteration, the client nodes first download the global model maintained by the PS, based on

which several rounds of local updates are performed using the private local data. The updated local models are then transmitted to the PS for global model aggregation. Nevertheless, as DL models, typically with millions of parameters, need to be uploaded to the Cloud in every global iteration, the communication latency caused by core-network congestion significantly bottlenecks the learning efficiency [4], [5].

Attributed to the emergence of mobile edge computing (MEC) [6], federated edge learning (FEEL), where an edge server located in close proximity to the client nodes (e.g., a base station) is deployed as the PS, was proposed as a promising remedy for Cloud-based FL [7]. Despite its great promise in reducing model uploading latency, one of the major challenges in FEEL systems is the unstable wireless connections between the client nodes and the edge PS, and client nodes with unfavorable channel conditions may become stragglers for model aggregation and in turn slow down the training process. As a result, improving the training efficiency of FEEL has drawn great interests in existing literature. Considering the limited resources, a control algorithm to determine the global model aggregation frequency of FEEL was developed in [8] to maximize the learning performance. In order to reduce the training time, a client selection algorithm was proposed for FEEL in [9], which eliminates the straggling client nodes from global model aggregation. Besides, gradient quantization and sparsification techniques were also adopted to achieve communication-efficient FEEL [10], [11]. However, the number of accessible client nodes of a single edge server is generally limited, which hinders the benefits of FL due to the small amount of training data.

To unleash the full potential of FEEL, recent works exploited cooperation among multiple edge servers for model training. In [12], a client-edge-cloud hierarchical FL system along with a training algorithm, namely HierFAVG, was developed, which takes advantages of the Cloud and edge servers to accelerate model training. Similar investigations in [13] extended HierFAVG to a multi-level stochastic gradient descent (SGD) algorithm. Besides, a fog-assisted FL framework was proposed in [14], where the Cloud-based PS selects an optimal fog node to serve as the global model aggregator in each communication round. Unfortunately, these works still rely on the connection to the Cloud, which may suffer from excessive communication latency. Besides, such architectures are vulnerable to single-point failure and not scalable to large-

scale deployment.

In this paper, we investigate a novel FL architecture, namely semi-decentralized federated edge learning (SD-FEEL), to improve the training efficiency. This architecture is motivated by the low communication latency between edge servers so that efficient model exchange can be realized. Specifically, we consider multiple edge servers, and each of them coordinates a cluster of client nodes to perform local model updating and *intra-cluster* model aggregation. The edge servers periodically share their updated models to the neighboring edge servers for *inter-cluster* model aggregation. Such a semi-decentralized training protocol can accelerate the learning process since a large number of client nodes can collaborate with low communication cost. It is worthy mentioning that a similar design was investigated in [15], which, however, was limited to an idealized independent and identically distributed (IID) assumption of the local training data. Our work in this paper advances SD-FEEL in the following aspects:

- We extend SD-FEEL to the case with non-IID data. To investigate impacts of the network topology on learning performance, the edge servers are allowed to share and aggregate models multiple times in each round of inter-cluster model aggregation.
- Convergence of a training algorithm supporting SD-FEEL on non-IID data is proved. Our analysis shows when both intra-cluster and inter-cluster model aggregations are performed at each iteration, SD-FEEL reduces to the vanilla SGD [16] given mutually connected edge servers. This is also achievable by multiple times of inter-server model sharings when the edge servers are only partially connected.
- Extensive experiments are conducted to demonstrate the benefits of SD-FEEL in achieving fast convergence compared to existing FL schemes. Our results also provide insightful guidelines on choosing the intra-/inter-cluster model aggregation frequencies and the communication strategy among edge servers to reduce the training latency.

The rest of the paper is organized as follows. Section II introduces the framework of semi-decentralized FEEL. Section III shows the convergence of SD-FEEL on non-IID data and discusses various insights. We present experiment results in Section IV and conclude this paper in Section V.

II. SEMI-DECENTRALIZED FEEL

In this section, we first introduce the semi-decentralized FEEL system, and a training algorithm is then presented.

A. Semi-Decentralized FEEL System

We consider an edge-assisted federated learning system as shown in Fig. 1, which consists of C client nodes (denoted as set \mathcal{C}) and D edge servers (denoted as set \mathcal{D}). Each client node is associated with an edge server according to some pre-defined criteria, e.g., physical proximity and network coverage. We denote the set of client nodes associated with the d -th edge server as \mathcal{C}_d , which form one edge cluster. Some of the edge servers are inter-connected via high-speed cables, which facilitates information exchange for SD-FEEL. We use

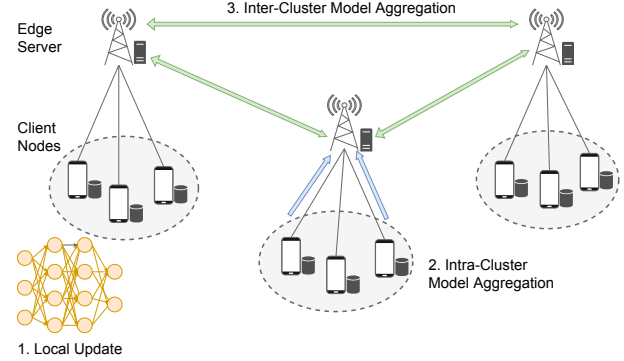


Fig. 1: Semi-decentralized FEEL system.

a connected graph \mathcal{G} to model the connectivity among the edge servers, and denote the one-hop neighbors of the d -th edge server as \mathcal{N}_d .

Each client node is assumed to have a set of local training data, denoted as $\mathcal{S}_i = \{\mathbf{x}_j, y_j\}_{j=1}^{|\mathcal{S}_i|}$, $i \in \mathcal{C}$, where \mathbf{x}_j is the data sample and y_j is the corresponding label. The whole training dataset and the collection of local training data across the client nodes associated with the d -th server are denoted as \mathcal{S} and \mathcal{S}'_d , respectively. The client nodes collaborate to train a shared DL model, denoted as $\mathbf{w} \in \mathbb{R}^M$ with M as the number of trainable parameters. Let $f(\mathbf{x}_j, y_j; \mathbf{w})$ be the loss function associated with the data sample (\mathbf{x}_j, y_j) based on the model \mathbf{w} . As a result, the objective of FL is to minimize the loss function over all the training data, i.e.,

$$\min_{\mathbf{w} \in \mathbb{R}^M} \left\{ F(\mathbf{w}) \triangleq \sum_{i \in \mathcal{C}} \frac{|\mathcal{S}_i|}{|\mathcal{S}|} F_i(\mathbf{w}) \right\}, \quad (1)$$

where $F_i(\mathbf{w}) \triangleq \frac{1}{|\mathcal{S}_i|} \sum_{j \in \mathcal{S}_i} f(\mathbf{x}_j, y_j; \mathbf{w})$.

It is important to note that we will not pose the assumption of homogeneous (i.e., IID) data across the client nodes, which is more reflective of real scenarios and also a highly non-trivial extension compared to the existing study [15].

B. Training Algorithm

Without loss of generality, we assume there are K iterations in the training process, which contains three main procedures, including 1) local model update, 2) intra-cluster model aggregation, and 3) inter-cluster model aggregation. While local model updates are performed at the client nodes, the edge servers are in charge of the other two procedures. The periods of intra-cluster and inter-cluster model aggregation, denoted as τ_1 and τ_2 respectively, are two critical hyper-parameters in the training algorithm.

1) *Local Model Update*: In the k -th iteration, each client node performs model update with its local data using the mini-batch SGD algorithm according to the following expression:

$$\mathbf{w}_k^{(i)} \leftarrow \mathbf{w}_{k-1}^{(i)} - \eta g(\xi_k^{(i)}; \mathbf{w}_{k-1}^{(i)}), i \in \mathcal{C}, \quad (2)$$

where $\mathbf{w}_{k-1}^{(i)}$ is the most updated model available at the i -th client node at the start of the k -th iteration, $g(\xi_k^{(i)}; \mathbf{w}_{k-1}^{(i)})$ is

the gradient computed on the batch of randomly-sampled local training data $\xi_k^{(i)}$, and η denotes the learning rate.

2) *Intra-cluster Model Aggregation*: In the k -th iteration (when k is a multiple integer of τ_1 but not $\tau_1\tau_2$), each client node uploads its most updated model to the associated edge server, and the edge server aggregates the received local models according to the following expression:

$$\tilde{\mathbf{w}}_k^{(d)} \leftarrow \sum_{i \in \mathcal{C}_d} \frac{|\mathcal{S}_i|}{|\mathcal{S}'_d|} \mathbf{w}_k^{(i)}, d \in \mathcal{D}, \quad (3)$$

where $\tilde{\mathbf{w}}_k^{(d)}$ denotes the intra-cluster aggregated model at the d -th edge server. After that, $\tilde{\mathbf{w}}_k^{(d)}$ is broadcasted to the client nodes \mathcal{C}_d , which can be expressed as follows:

$$\mathbf{w}_k^{(i)} \leftarrow \tilde{\mathbf{w}}_k^{(d)}, i \in \mathcal{C}_d. \quad (4)$$

3) *Inter-cluster Model Aggregation*: In the k -th iteration (when k is a multiple integer of $\tau_1\tau_2$), after intra-cluster model aggregation, each edge server also shares its intra-cluster aggregated model to the one-hop neighbouring edge servers for inter-cluster model aggregation, before sending it back to the client nodes. Each round of inter-cluster model aggregation consists $\alpha \in \{1, 2, \dots\}$ times of model sharing and aggregation, which can be expressed as follows:

$$\hat{\mathbf{w}}_{k,l}^{(d)} \leftarrow \sum_{j \in \mathcal{N}_d \cup \{d\}} p_{d,j} \hat{\mathbf{w}}_{k,l-1}^{(j)}, l = 1, 2, \dots, \alpha, \quad (5)$$

where $\hat{\mathbf{w}}_{k,0}^{(d)} = \tilde{\mathbf{w}}_k^{(d)}$ is the intra-cluster aggregated model at the d -th edge server, and $\mathbf{P} \triangleq [p_{i,j}] \in \mathbb{R}^{D \times D}$ is termed as the mixing matrix. We choose \mathbf{P} according to the following criterion that can achieve fast linear iterative averaging in [17]:

$$\mathbf{P} = \mathbf{I} - \frac{2}{\lambda_1(\mathbf{L}) + \lambda_{D-1}(\mathbf{L})} \mathbf{L}, \quad (6)$$

where \mathbf{I} is the identity matrix, \mathbf{L} is the Laplacian matrix of graph \mathcal{G} , and $\lambda_i(\mathbf{L})$ denotes the i -th largest eigenvalue of matrix \mathbf{L} . Once $\hat{\mathbf{w}}_{k,\alpha}^{(d)}$ is computed, it updates $\tilde{\mathbf{w}}_k^{(d)}$ as $\hat{\mathbf{w}}_{k,\alpha}^{(d)}$, which is then transmitted to the client nodes in \mathcal{C}_d . Details of the training algorithm are summarized in Algorithm 1, where K is assumed to be an integral multiple of $\tau_1\tau_2$.

III. CONVERGENCE ANALYSIS FOR SD-FEEL

In this section, we prove the convergence of Algorithm 1, and draw various insights from our analysis.

A. Assumptions

We make the following assumptions on the loss functions to facilitate the convergence analysis.

Assumption 1. For all $i \in \mathcal{C}$, we assume:

- **(Smoothness)** The objective function is L -smooth, i.e.,

$$\|\nabla F_i(\mathbf{w}_1) - \nabla F_i(\mathbf{w}_2)\|_2 \leq L \|\mathbf{w}_1 - \mathbf{w}_2\|_2, \forall \mathbf{w}_1, \mathbf{w}_2 \in \mathbb{R}^M. \quad (7)$$

- **(Unbiased and bounded gradient variance)** The mini-batch gradient $g(\xi; \mathbf{w})$ is unbiased, i.e.,

$$\mathbb{E}_{\xi|\mathbf{w}}[g(\xi; \mathbf{w})] = \nabla F_i(\mathbf{w}), \forall \mathbf{w} \in \mathbb{R}^M, \quad (8)$$

Algorithm 1 Training Algorithm for SD-FEEL

```

1: Initialize all client nodes with same model, i.e.,  $\mathbf{w}_0^{(i)} = \mathbf{w}_0, i \in \mathcal{C}$ .
2: for  $k = 1, 2, \dots, K$  do
3:   for each client node  $i \in \mathcal{C}$  in parallel do
4:     Update the local model as  $\mathbf{w}_k^{(i)}$  according to (2);
5:     if  $\text{mod}(k, \tau_1) = 0$  then
6:       for each edge server  $d \in \mathcal{D}$  in parallel do
7:         Collect the most updated model from the client
           nodes in  $\mathcal{C}_d$ ;
8:         Obtain  $\tilde{\mathbf{w}}_k^{(d)}$  by performing intra-cluster model
           aggregation according to (3);
9:         if  $\text{mod}(k, \tau_1\tau_2) = 0$  then
10:          Set  $\hat{\mathbf{w}}_{k,0}^{(d)}$  as  $\tilde{\mathbf{w}}_k^{(d)}$ ;
11:          for  $l = 1, \dots, \alpha$  do
12:            Send the most updated model  $\hat{\mathbf{w}}_{k,l-1}^{(d)}$  to its
           one-hop neighbors  $\mathcal{N}_d$ ;
13:            Receive models from  $\mathcal{N}_d$  and perform inter-
           cluster model aggregation according to (5);
14:          end for
15:          Update  $\hat{\mathbf{w}}_k^{(d)}$  as  $\hat{\mathbf{w}}_{k,\alpha}^{(d)}$ ;
16:        end if
17:        Broadcast  $\hat{\mathbf{w}}_k^{(d)}$  to the client nodes in  $\mathcal{C}_d$ ;
18:      end for
19:    end if
20:  end for
21: end for

```

and there exists $\sigma > 0$ such that

$$\mathbb{E}_{\xi|\mathbf{w}} \left[\|g(\xi; \mathbf{w}) - \nabla F_i(\mathbf{w})\|_2^2 \right] \leq \sigma^2, \forall \mathbf{w} \in \mathbb{R}^M. \quad (9)$$

- **(Degree of non-IIDness)** There exists $\kappa > 0$ such that

$$\|\nabla F_i(\mathbf{w}) - \nabla F(\mathbf{w})\|_2 \leq \kappa, \quad \forall \mathbf{w} \in \mathbb{R}^M. \quad (10)$$

When $\kappa = 0$, $\nabla F(\mathbf{w}) = \nabla F_i(\mathbf{w}), \forall i \in \mathcal{C}$, which reduces to the case of IID data across the client nodes.

B. Convergence Analysis

Denote $\mathbf{W}_k \triangleq [\mathbf{w}_k^{(i)}] \in \mathbb{R}^{M \times C}$ and $\mathbf{G}_k \triangleq [g(\xi_{k+1}; \mathbf{w}_k^{(i)})] \in \mathbb{R}^{M \times C}$. To characterize the evolution of \mathbf{W}_k as shown in the following lemma, we define $\mathbf{H}' \triangleq [h'_{i,d}] \in \mathbb{R}^{C \times D}$ and $\mathbf{H}'' \triangleq [h''_{d,i}] \in \mathbb{R}^{D \times C}$, where $h'_{i,d} = \frac{|\mathcal{S}_i|}{|\mathcal{S}'_d|} \mathbb{1}\{i \in \mathcal{C}_d\}$, $h''_{d,i} = \mathbb{1}\{i \in \mathcal{C}_d\}$, and $\mathbb{1}\{\cdot\}$ is the indicator function.

Lemma 1. The local models evolve according to the following expression:

$$\mathbf{W}_{k+1} = (\mathbf{W}_k - \eta \mathbf{G}_k) \mathbf{T}_k, k = 0, 1, \dots, K-1, \quad (11)$$

where

$$\mathbf{T}_k = \begin{cases} \mathbf{H}' \mathbf{H}'' & \text{if } \text{mod}(k, \tau_1) = 0 \text{ and } \text{mod}(k, \tau_1\tau_2) \neq 0, \\ \mathbf{H} \mathbf{P}^\alpha \mathbf{H}'' & \text{if } \text{mod}(k, \tau_1\tau_2) = 0, \\ \mathbf{I}, & \text{otherwise.} \end{cases} \quad (12)$$

Proof. The proof can be obtained by rewriting (5) as $\hat{\mathbf{W}}_{k,l} = \mathbf{P}\hat{\mathbf{W}}_{k,l-1}$ and showing $\hat{\mathbf{W}}_{k,\alpha} = \mathbf{P}^\alpha\hat{\mathbf{W}}_{k,0}$. Details are omitted for brevity. \square

For convenience, we define $\mathbf{u}_k \triangleq \sum_{i \in \mathcal{C}} m_i \mathbf{w}_k^{(i)}$ where $m_i \triangleq \frac{|\mathcal{S}_i|}{|\mathcal{S}|}$, and $\|\mathbf{X}\|_{\mathbf{M}} \triangleq \sum_{i=1}^M \sum_{j=1}^N m_{i,j} |x_{i,j}|^2$ is the weighted Frobenius norm of an $M \times N$ matrix \mathbf{X} . Following Lemma 8 in [18] and leveraging the evolution expression of \mathbf{W}_k in (11), we bound the expected change of the loss functions in consecutive iterations as follows:

$$\begin{aligned} \mathbb{E}[F(\mathbf{u}_{k+1})] - \mathbb{E}[F(\mathbf{u}_k)] &\leq -\frac{\eta}{2} \mathbb{E} \left[\|\nabla F(\mathbf{u}_k)\|_2^2 \right] + \frac{L\eta^2}{2C} \sigma^2 \\ &\quad - \left(\frac{\eta}{2} - \frac{\eta^2 LC}{2} \right) J_k + \frac{\eta L^2}{2} \mathbb{E} \left[\|\mathbf{W}_k(\mathbf{I} - \mathbf{M})\|_{\mathbf{M}}^2 \right], \end{aligned} \quad (13)$$

where $\mathbf{M} \triangleq \mathbf{m}\mathbf{1}^T$ and $J_k \triangleq \sum_{i \in \mathcal{C}} m_i \mathbb{E} \left[\left\| \nabla F_i(\mathbf{w}_k^{(i)}) \right\|_2^2 \right]$. It remains to bound the last term in the right-hand side (RHS) of (13) in order to show the convergence of Algorithm 1, which can be interpreted as the deviation of the local models from their mean, as shown in Lemma 2.

Lemma 2. *With Assumption 1, we have:*

$$\begin{aligned} \frac{1}{K} \sum_{k=1}^K \mathbb{E} \left[\|\mathbf{W}_k(\mathbf{I} - \mathbf{M})\|_{\mathbf{M}}^2 \right] &\leq 2\eta^2 V_1 (\sigma^2 + \kappa^2) \\ &\quad + 2\eta^2 V_2 \sum_{i \in \mathcal{C}} m_i^2 \kappa^2 + \frac{2\eta^2 V_2}{K} \sum_{k=1}^K J_k, \end{aligned} \quad (14)$$

where $\zeta = |\lambda_2(\mathbf{P})| \in [0, 1]$, $\Lambda = \frac{\zeta^{2\alpha}}{1-\zeta^{2\alpha}} + \frac{2\zeta^\alpha}{1-\zeta^\alpha} + \frac{\zeta^{2\alpha}}{(1-\zeta^\alpha)^2}$, $V_1 = \tau_1^2 \tau_2^2 \sum_{i \in \mathcal{C}} m_i \left[\Lambda + \frac{2-\zeta^\alpha}{1-\zeta^\alpha} \left(\tau_1^2 \frac{(\tau_2-1)(2\tau_2+1)}{6} + \frac{(\tau_1-1)(2\tau_1+1)}{6} \right) \right]$, and $V_2 = \tau_1^2 \tau_2^2 \left(\Lambda + \frac{2(\tau_1-1)}{\tau_1} \right)$.

Proof. By using (11), we expand $\mathbf{W}_k(\mathbf{I} - \mathbf{M})$ as $\mathbf{W}_0(\mathbf{I} - \mathbf{M}) \prod_{l=0}^{k-1} \mathbf{T}_l - \eta \sum_{s=0}^{k-1} \mathbf{G}_s \left(\prod_{l=s}^{k-1} \mathbf{T}_l - \mathbf{M} \right)$. Since $\mathbf{w}_0^{(i)} = \mathbf{w}_0, \forall i \in \mathcal{C}$, (14) can be shown by bounding $\mathbb{E} \left[\left\| \eta \sum_{s=0}^{k-1} \mathbf{G}_s \left(\prod_{l=s}^{k-1} \mathbf{T}_l - \mathbf{M} \right) \right\|_{\mathbf{M}}^2 \right]$. Please refer to Appendix C for the complete proof. \square

By substituting (12) in the RHS of (11) and choosing a proper learning rate to eliminate the term $\frac{1}{K} \sum_{k=1}^K J_k$, we are able to bound the expected average-square gradients in the following theorem.

Theorem 1. *If the learning rate η satisfies:*

$$1 - LC\eta - 2L^2\eta^2 V_2 \geq 0, \quad (15)$$

we have:

$$\begin{aligned} \frac{1}{K} \sum_{k=1}^K \mathbb{E} \left[\|\nabla F(\mathbf{u}_k)\|_2^2 \right] &\leq \frac{2\Delta}{\eta K} + L\eta \sum_{i \in \mathcal{C}} m_i^2 \sigma^2 \\ &\quad + 2L^2\eta^2 V_1 \sigma^2 + 2L^2\eta^2 (V_1 + V_2 \sum_{i \in \mathcal{C}} m_i^2) \kappa^2, \end{aligned} \quad (16)$$

where $\Delta \triangleq \mathbb{E}[F(\mathbf{u}_1)] - \mathbb{E}[F(\mathbf{u}^*)]$ and $\mathbf{u}^* \triangleq \arg \min_{\mathbf{w}} F(\mathbf{w})$.

Proof. Please refer to the Appendix D. \square

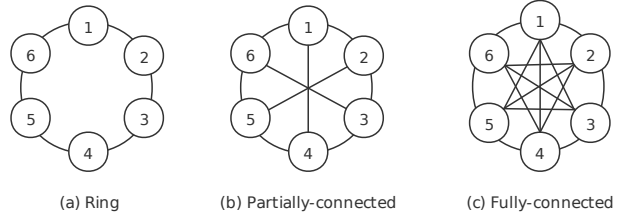


Fig. 2: Typical network topologies of the edge servers.

Corollary 1. *If the learning rate is chosen as $\eta = \frac{1}{L} \sqrt{\frac{1}{K \sum_{i \in \mathcal{C}} m_i^2}}$, (16) can be simplified as follows:*

$$\begin{aligned} \frac{1}{K} \sum_{k=1}^K \mathbb{E} \left[\|\nabla F(\mathbf{u}_k)\|_2^2 \right] &\leq \frac{(2L\Delta + \sigma^2) \sqrt{\sum_{i \in \mathcal{C}} m_i^2}}{\sqrt{K}} \\ &\quad + \frac{1}{K} \left[\frac{2V_1}{\sum_{i \in \mathcal{C}} m_i^2} \sigma^2 + \left(\frac{2V_1}{\sum_{i \in \mathcal{C}} m_i^2} + 2V_2 \right) \kappa^2 \right], \end{aligned} \quad (17)$$

which implies Algorithm 1 converges within $\mathcal{O}(\frac{1}{\epsilon^2})$ training iterations (ϵ denotes the desired training accuracy).

With the results in Theorem 1, we are able to draw various insights as elaborated in the following remarks.

Remark 1. It is straightforward that the RHS of (16) increases with both τ_1 and τ_2 . Thus, it is preferable to choose $\tau_1 = \tau_2 = 1$ to reduce the number of training iterations without considering training time. However, as will be seen in Section IV, performing either intra-cluster or inter-cluster model aggregations most frequently turns out to be sub-optimal for training latency reduction.

Remark 2. By taking first-order derivative, we see that the RHS of (16) also decreases with ζ^α , indicating that either increasing α (i.e., increasing the inter-server communication overhead) or decreasing ζ (i.e., increasing the degree of connectivity among the edge servers) results in faster convergence. To better illustrate, three typical network topologies of six edge servers are shown in Fig. 2, including the ring, partially connected and fully connected topologies, and the values of ζ are given as 0.6, 0.333 and 0, respectively. Besides, in extreme cases with $\alpha \rightarrow \infty$, the edge servers can reach consensus after inter-cluster model aggregation (i.e., $\tilde{\mathbf{w}}_k^{(d)} \rightarrow \frac{1}{D} \sum_{j \in \mathcal{D}} \tilde{\mathbf{w}}_k^{(j)}$) even with a sparsely connected network.

Remark 3. When $\tau_1 = 1$, $\tau_2 = 1$, and $\zeta^\alpha = 0$, i.e., the local models of all the client nodes are synchronized at each iteration, the convergence result in Theorem 1 reduces to that of the fully synchronous SGD algorithm [16]. In addition, when $\kappa = 0$, i.e., in the IID case, our result also improves over that obtained in [15].

IV. EXPERIMENTS

A. Settings

We simulate an SD-FEEL system with 50 client nodes and 10 edge servers, and each edge server is associated with five

client nodes. We consider the partially connected network topology as shown in Fig. 2(b) unless otherwise specified.

SD-FEEL is evaluated on two benchmark datasets for image classification, including the MNIST [19] and CIFAR-10 [20] datasets, both of which contain ten categories of images. For non-IID data distribution, we adopt the skewed label partition [21] where each client node possesses only one random class of images. We use a convolutional neural network (CNN) with two 5×5 convolution layers as proposed in [3] for MNIST, and adopt a standard ResNet-18 [22] for CIFAR-10, which have 21,840 and 11,173,962 trainable parameters, respectively. In mini-batch SGD, 0.001 and 0.01 are the learning rates for MNIST and CIFAR-10, respectively, and the batch size is set as 10.

To verify the benefits of SD-FEEL in reducing training latency, we adopt the following FL schemes for comparisons:

- FedAvg [3]: This is a Cloud-based FL scheme, where a Cloud-based PS collects and aggregates models from all client nodes after every $\tau = \tau_1 \tau_2$ local model updates.
- HierFAVG [12]: This FL scheme leverages a Cloud-based PS and multiple edge servers. Specifically, the edge servers perform local model aggregation after every τ_1 local updates; whereas the Cloud-based PS aggregates models from the edge servers after every τ_2 local model aggregations.

B. Training Latency Calculation

For SD-FEEL, the latency of K training iterations can be evaluated using the following expression:

$$t_{\text{tot}} = \left\lceil \frac{K}{\tau_1 \tau_2} \right\rceil [\tau_2 (\tau_1 t_{\text{comp}}^{\text{ct}} + t_{\text{comm}}^{\text{ct-sr}}) + \alpha t_{\text{comm}}^{\text{sr-sr}}],$$

where $t_{\text{comp}}^{\text{ct}}$ denotes the computation latency for each local update, $t_{\text{comm}}^{\text{ct-sr}}$ denotes the model uploading latency between a client node and its associated edge server, and $t_{\text{comm}}^{\text{sr-sr}}$ is the model transmission latency between neighboring edge servers. Following [12], we assume $t_{\text{comp}}^{\text{ct}} = \frac{c D_s}{f}$, where $f = 2$ GHz is the processing speed of the client nodes, D_s is the size of training data given by 62,720 and 245,760 bits for MNIST and CIFAR-10, respectively. Considering the computation complexity of training different DL models, we set c as 20 and 10,230 cycles/bit for the adopted CNN and ResNet-18, respectively. It is also assumed that the client nodes communicate with the associated edge servers using orthogonal channels without inter-cluster interference, and thus the model uploading latency is given by $t_{\text{comm}}^{\text{ct-sr}} = \frac{M \times 32 \text{ bits/parameter}}{B \log_2 (1 + \text{SNR})}$ with $B = 1$ MHz and $\text{SNR} \approx 17$ dB. The transmission rate between neighboring edge servers is set to be 1/10 of that between the client nodes and the edge server, i.e., $t_{\text{comm}}^{\text{sr-sr}} = 0.1 t_{\text{comm}}^{\text{ct-sr}}$. Given the core-network congestion, model uploading latency from client nodes or edge servers to the Cloud-based PS is set to be 10 times of $t_{\text{comm}}^{\text{ct-sr}}$ in FedAvg and HierFAVG.

C. Results

1) *Convergence Speed and Learning Performance*: We show the training loss over time on the MNIST and CIFAR-10 datasets in Fig. 3(a) and Fig. 3(b), respectively. For both tasks,

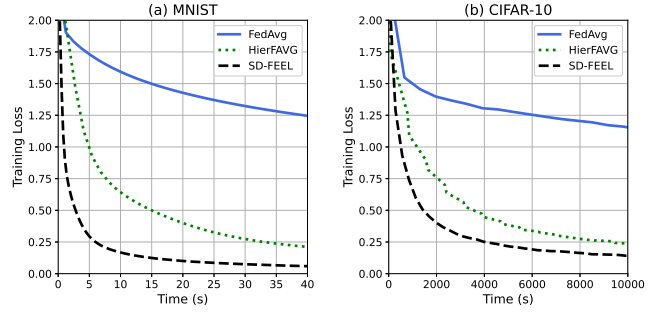


Fig. 3: Training loss over time on (a) MNIST ($\alpha = 1$, $\tau_1 = 5$, and $\tau_2 = 1$) and (b) CIFAR-10 ($\alpha = 1$, $\tau_1 = 5$, and $\tau_2 = 2$).

TABLE I: TEST ACCURACY

Dataset (Time)	FedAvg	HierFAVG	SD-FEEL
MNIST (40s)	62.62%	92.19%	96.61%
CIFAR-10 (10000s)	60.82%	90.28%	91.20%

it can be observed that, the training loss of SD-FEEL drops rapidly at early stage of the training process, and converges at around 40s and 10000s for the MNIST and CIFAR-10 datasets, respectively. While the progress of FedAvg lags far behind due to model uploading from the client nodes to the Cloud-based PS in each iteration, the training loss of HierFAVG is significantly higher than that of SD-FEEL even with much less frequent communications to the Cloud. This verifies the effectiveness of SD-FEEL in achieving fast convergence without relying on the Cloud-based infrastructure.

The learning performance of SD-FEEL, HierFAVG and FedAvg in terms of test accuracy are compared in Table I. It is seen that SD-FEEL secures noticeable performance improvements compared to HierFAVG, while the learned models of FedAvg within the given training time are simply unusable.

2) *Ablation Study*: We investigate impacts of the intra-cluster model aggregation period τ_1 by showing the relationship between training loss and iterations (training latency) in Fig. 4(a) (Fig. 4(b)). For both figures, we fix τ_2 to 1 and evaluate the configurations with $\tau_1 = 1, 5$ and 10. It is observed from Fig. 4(a) that a smaller value of τ_1 leads to lower training loss within a given number of training iterations, as discussed in Remark 1. However, this conclusion becomes invalid in terms of training latency as shown in Fig. 4(b), where $\tau_1 = 5$ achieves the minimum training loss. This is owing to the fact that less frequent intra-cluster model aggregations help to save communication time. Similar behaviors can be observed by varying τ_2 with a given value of τ_1 . We omit the results here due to the limited space. These observations jointly necessitate an optimal choice of the intra-cluster and inter-cluster model aggregation frequencies for training latency reduction in SD-FEEL.

We also evaluate the test accuracy of SD-FEEL on different network topologies of the edge servers in Fig. 5(a). We see that within a given number of training iterations, a more connected

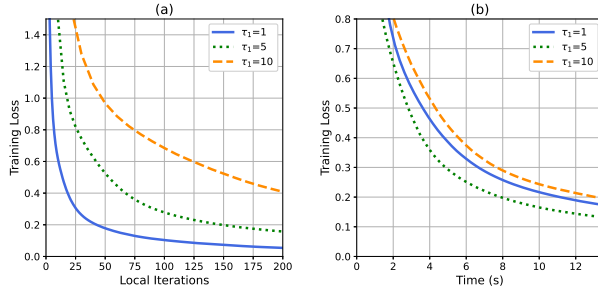


Fig. 4: Training loss of SD-FEEL vs. (a) iterations and (b) time on the MNIST dataset ($\alpha = 1$ and $\tau_2 = 1$).

network topology achieves higher test accuracy, since more information is collected from neighboring edge clusters in each round of inter-server model aggregation, as explained in Remark 2. Besides, effects of α on test accuracy are examined via a ring topology in Fig. 5(b). In line with Remark 2, a larger value of α increases the training speed in terms of iterations. It can also be observed that when α is greater than 5, the test accuracy approaches the case with a fully-connected network, and further increasing α brings marginal improvement. Therefore, based on the network topology of edge servers, we can choose different values of α to balance the communication cost and learning performance.

V. CONCLUSIONS

In this paper, we investigated a novel FL architecture, namely semi-decentralized federated edge learning (SD-FEEL) to realize low-latency distributed learning on non-IID data. Convergence analysis was conducted for the training algorithm of SD-FEEL, from which, various insights were drawn for system implementation. Simulations demonstrated that SD-FEEL substantially reduces the training latency while improving the learning performance. For future work, it is worth investigating the optimal intra-cluster and inter-cluster model aggregation frequencies and considering more practical scenarios with device heterogeneity.

REFERENCES

- [1] K. L. Lueth, “State of the IoT 2020: 12 billion IoT connections, surpassing non-IoT for the first time,” Nov. 2020. [Online]. Available: <https://iot-analytics.com/state-of-the-iot-2020-12-billion-iot-connections-surpassing-non-iot-for-the-first-time/>.
- [2] F. Meneghelli, M. Calore, D. Zucchetto, M. Polese, and A. Zanella, “IoT: Internet of Threats? A survey of practical Security Vulnerabilities in Real IoT Devices,” *IEEE Internet Things J.*, vol. 6, no. 5, pp. 8182–8201, Oct. 2019.
- [3] B. McMahan, E. Moore, D. Ramage, S. Hampson, and B. A. y Arcas, “Communication-efficient learning of deep networks from decentralized data,” in *Proc. Int. Conf. Artif. Intell. Statist. (AISTATS)*, Ft. Lauderdale, FL, USA, Apr. 2017.
- [4] T. Li, A. K. Sahu, A. Talwalkar, and V. Smith, “Federated learning: Challenges, methods, and future directions,” *IEEE Signal Process. Mag.*, vol. 37, no. 3, pp. 50–60, May 2020.
- [5] Y. Shi, K. Yang, T. Jiang, J. Zhang, and K. B. Letaief, “Communication-Efficient Edge AI: Algorithms and Systems,” *IEEE Commun. Surveys Tuts.*, vol. 22, no. 4, pp. 2167–2191, 4th Quart., Jul. 2020.
- [6] Y. Mao, C. You, J. Zhang, K. Huang, and K. B. Letaief, “A survey on mobile edge computing: The communication perspective,” *IEEE Commun. Surveys Tuts.*, vol. 19, no. 4, pp. 2322–2358, 4th Quart., Aug. 2017.
- [7] W. Y. B. Lim *et al.*, “Federated learning in mobile edge networks: A comprehensive survey,” *IEEE Commun. Surveys Tuts.*, vol. 22, no. 3, pp. 2031–2063, 3rd Quart., Apr. 2020.
- [8] S. Wang *et al.*, “Adaptive federated learning in resource constrained edge computing systems,” *IEEE J. Sel. Areas Commun.*, vol. 37, no. 6, pp. 1205–1221, Mar. 2019.
- [9] T. Nishio and R. Yonetani, “Client selection for federated learning with heterogeneous resources in mobile edge,” in *Proc. IEEE Int. Conf. Commun. (ICC)*, Shanghai, China, May 2019.
- [10] J. Mills, J. Hu, and G. Min, “Communication-efficient federated learning for wireless edge intelligence in IoT,” *IEEE Internet Things J.*, vol. 7, no. 7, pp. 5986–5994, Jul. 2020.
- [11] M. M. Amiri and D. Gündüz, “Federated learning over wireless fading channels,” *IEEE Trans. Wireless Commun.*, vol. 19, no. 5, pp. 3546–3557, Feb. 2020.
- [12] L. Liu, J. Zhang, S. Song, and K. B. Letaief, “Client-edge-cloud hierarchical federated learning,” in *Proc. IEEE Int. Conf. Commun. (ICC)*, Dublin, Ireland, Jun. 2020.
- [13] J. Wang, S. Wang, R.-R. Chen, and M. Ji, “Local averaging helps: Hierarchical Federated Learning and Convergence Analysis,” *arXiv preprint arXiv:2010.12998*, Oct. 2020.
- [14] R. Saha, S. Misra, and P. K. Deb, “FogFL: Fog Assisted Federated Learning for Resource-Constrained IoT Devices,” *IEEE Internet Things J.*, to appear.
- [15] T. Castiglia, A. Das, and S. Patterson, “Multi-Level Local SGD for Heterogeneous Hierarchical Networks,” *arXiv preprint arXiv:2007.13819*, Jul. 2020.
- [16] L. Bottou, F. E. Curtis, and J. Nocedal, “Optimization methods for large-scale machine learning,” *SIAM Rev.*, vol. 60, no. 2, pp. 223–311, Aug. 2018.
- [17] L. Xiao and S. Boyd, “Fast linear iterations for distributed averaging,” *Syst. Control Lett.*, vol. 53, no. 1, pp. 65–78, Sep. 2004.
- [18] H. Tang, X. Lian, M. Yan, C. Zhang, and J. Liu, “D²: Decentralized training over decentralized data,” in *Proc. Int. Conf. Mach. Learn. (ICML)*, Stockholm, Sweden, Jul. 2018.
- [19] Y. LeCun, L. Bottou, Y. Bengio, and P. Haffner, “Gradient-based learning applied to document recognition,” *Proc. IEEE*, vol. 86, no. 11, pp. 2278–2324, Nov. 1998.
- [20] A. Krizhevsky *et al.*, “Learning multiple layers of features from tiny images,” *Citeseer*, Tech. Rep., Apr. 2009.
- [21] K. Hsieh, A. Phanishayee, O. Mutlu, and P. Gibbons, “The non-iid data quagmire of decentralized machine learning,” in *Proc. Int. Conf. Mach. Learn. (ICML)*, Virtual Event, Jul. 2020.
- [22] K. He, X. Zhang, S. Ren, and J. Sun, “Deep residual learning for image recognition,” in *Proc. IEEE Conf. Comput. Vision Pattern Recogn. (CVPR)*, Las Vegas, NV, USA, Jun. 2016.

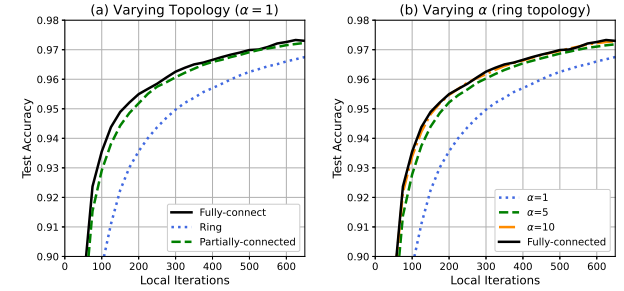


Fig. 5: Test accuracy on the MNIST dataset ($\tau_1 = 5, \tau_2 = 5$) with (a) different network topologies and (b) different values of α .

APPENDIX

A. Notations

We denote $m_i \triangleq \frac{|\mathcal{S}_i|}{|\mathcal{S}|}$, $\mathbf{m} \triangleq [m_i] \in \mathbb{R}^C$, $\mathbf{M} \triangleq \mathbf{m}\mathbf{1}^T$, $\mathbf{H}_1 \triangleq \mathbf{H}'\mathbf{H}''$, $\mathbf{H}_2 \triangleq \mathbf{H}'\mathbf{P}^\alpha\mathbf{H}''$, $J_k \triangleq \sum_{i \in \mathcal{C}} m_i \mathbb{E} \left\| \nabla F_i(\mathbf{w}_k^{(i)}) \right\|^2$, and $\mathbf{Z}_k \triangleq \left[\nabla F_i(\mathbf{w}_k^{(1)}), \dots, \nabla F_i(\mathbf{w}_k^{(C)}) \right]$.

The weighted sum of mini-batch stochastic gradients and local loss functions are defined respectively as follows:

$$\mathcal{G}_k \triangleq \mathbf{G}_k \mathbf{m} = \sum_{i \in \mathcal{C}} m_i g(\mathbf{w}_k^{(i)}), \quad \mathcal{Z}_k \triangleq \mathbf{Z}_k \mathbf{m} = \sum_{i \in \mathcal{C}} m_i \nabla F_i(\mathbf{w}_k^{(i)}). \quad (18)$$

We also define the accumulated stochastic gradient and derivative of the global loss function as follows:

$$Y_{j,l}^{(1)} \triangleq \sum_{s=j\tau_2\tau_1+1}^{j\tau_2\tau_1+l\tau_1} \mathbf{G}_s, \quad Y_{j,l,f}^{(2)} \triangleq \sum_{s=j\tau_2\tau_1+l\tau_1+1}^{j\tau_2\tau_1+l\tau_1+f} \mathbf{G}_s, \quad Y_r \triangleq \sum_{s=r\tau_2\tau_1+1}^{(r+1)\tau_2\tau_1} \mathbf{G}_s, \quad (19)$$

$$Q_{j,l}^{(1)} \triangleq \sum_{s=j\tau_2\tau_1+1}^{j\tau_2\tau_1+l\tau_1} \nabla F(\mathbf{X}_s), \quad Q_{j,l,f}^{(2)} \triangleq \sum_{s=j\tau_2\tau_1+l\tau_1+1}^{j\tau_2\tau_1+l\tau_1+f} \nabla F(\mathbf{X}_s), \quad Q_r \triangleq \sum_{s=r\tau_2\tau_1+1}^{(r+1)\tau_2\tau_1} \nabla F(\mathbf{X}_s). \quad (20)$$

B. Lemmas

Lemma 3. *The eigenvalues of \mathbf{H}_1 and \mathbf{H}_2 have the following properties:*

- \mathbf{H}_1 has a left eigenvector $\mathbf{1}^T$ with eigenvalue 1, and a right eigenvector \mathbf{m} with eigenvalue 1.
- \mathbf{H}_2 has a left eigenvector $\mathbf{1}^T$ with eigenvalue 1, and a right eigenvector \mathbf{m} with eigenvalue 1.
- The eigenvalues of \mathbf{H}_2 are same as the eigenvalues of \mathbf{P}^α , and the absolute values of all the eigenvalues except the largest one are no greater than 1.

Proof. Since when $\alpha = 0$, \mathbf{H}_2 reduces to \mathbf{H}_1 , it suffices to prove the first and second properties for \mathbf{H}_2 for arbitrary α . According to the definition of $\mathbf{H}_2 \triangleq \left[h_{i,j}^{(2)} \right] \in \mathbb{R}^{C \times C}$, we have:

$$h_{i,j}^{(2)} = \sum_{d'} \left(\sum_d h'_{i,d} p'_{d,d'} \right) h''_{d',j} \stackrel{(a)}{=} h'_{i,d(i)} p'_{d(i),d(j)} h''_{d(j),j} = \frac{|\mathcal{S}_i|}{|\mathcal{S}'_{d(i)}|} p'_{d(i),d(j)}, \quad (21)$$

where (a) holds since $h'_{i,d} = \frac{|\mathcal{S}_i|}{|\mathcal{S}'_d|} \mathbb{1}\{i \in \mathcal{C}_d\}$ and $h''_{d,i} = \mathbb{1}\{i \in \mathcal{C}_d\}$. Since $\sum_i h_{i,j}^{(2)} = 1$, it is easy to verify that \mathbf{H}_2 has a left eigenvector $\mathbf{1}^T$ with eigenvalue 1. Similarly, since $\sum_j h_{i,j}^{(2)} m_i = 1$, \mathbf{H}_2 has a right eigenvector \mathbf{m} with eigenvalue 1.

By invoking Proposition 2 of [15], it can be shown that the non-zero eigenvalues of \mathbf{H}_2 are same as those of \mathbf{P}^α . Since \mathbf{P} is doubly stochastic, i.e., it satisfies $\mathbf{P}^T = \mathbf{P}$ and $\mathbf{P}\mathbf{1} = \mathbf{1}$, the D eigenvalues satisfy $1 = |\lambda_1(\mathbf{P})| > |\lambda_2(\mathbf{P})| \geq \dots \geq |\lambda_D(\mathbf{P})| \geq 0$. Because $\lambda_i(\mathbf{P}^\alpha) = \lambda_i^\alpha(\mathbf{P})$, $i = 1, \dots, D$, we have $1 = |\lambda_1(\mathbf{P}^\alpha)| > |\lambda_2(\mathbf{P}^\alpha)| \geq \dots \geq |\lambda_D(\mathbf{P}^\alpha)| \geq 0$. \square

Lemma 4. *Matrix \mathbf{T}_k in (12) satisfies $\mathbf{T}_k \mathbf{M} = \mathbf{M} \mathbf{T}_k = \mathbf{M}$.*

Proof. We show this lemma by analyzing the three cases of (12) respectively. For the first case, we have $\mathbf{T}_k \mathbf{M} = \mathbf{H}'\mathbf{H}''\mathbf{M} = \mathbf{H}_1 \mathbf{m}^T = \mathbf{m}^T = \mathbf{M}$, and $\mathbf{M} \mathbf{T}_k = \mathbf{M} \mathbf{H}'\mathbf{H}'' = \mathbf{m}^T \mathbf{H}_1 = \mathbf{m}^T = \mathbf{M}$. For the second case, we have $\mathbf{T}_k \mathbf{M} = \mathbf{H}'\mathbf{P}^\alpha\mathbf{H}''\mathbf{M} = \mathbf{H}_2 \mathbf{m}^T = \mathbf{m}^T = \mathbf{M}$, and $\mathbf{M} \mathbf{T}_k = \mathbf{M} \mathbf{H}'\mathbf{P}^\alpha\mathbf{H}'' = \mathbf{m}^T \mathbf{H}_2 = \mathbf{m}^T = \mathbf{M}$. Moreover, the third case can be shown by similar arguments, i.e. $\mathbf{T}_k \mathbf{M} = \mathbf{I}\mathbf{M} = \mathbf{M}$ and $\mathbf{M} \mathbf{T}_k = \mathbf{M}\mathbf{I} = \mathbf{M}$. \square

Lemma 5. *The expected change of the global loss functions in consecutive iterations can be bounded as follows:*

$$\begin{aligned} \mathbb{E}F(\mathbf{u}_{k+1}) - \mathbb{E}F(\mathbf{u}_k) &\leq -\frac{\eta}{2} \mathbb{E} \left\| \nabla F(\mathbf{u}_k) \right\|^2 - \frac{\eta}{2} (1 - LC\eta) \sum_{i \in \mathcal{C}} m_i \mathbb{E} \left\| \nabla F_i(\mathbf{w}_k^{(i)}) \right\|^2 \\ &\quad + \frac{\eta L^2}{2} \mathbb{E} \left\| \mathbf{W}_k(\mathbf{I} - \mathbf{M}) \right\|_{\mathbf{M}}^2 + \frac{L\eta^2}{2} \sum_{i \in \mathcal{C}} m_i^2 \sigma^2, \end{aligned} \quad (22)$$

where $\|\cdot\|$ denotes the l_2 -vector norm.

Proof. First, we right multiply both sides of the evolution expression in (11) by \mathbf{M} , yielding the following expression:

$$\mathbf{u}_{k+1} = \mathbf{u}_k - \eta \mathcal{G}_k. \quad (23)$$

We apply the global loss function to both sides of (23), and due to the L -smoothness, we have:

$$\begin{aligned}
\mathbb{E}F(\mathbf{u}_{k+1}) &\leq \mathbb{E}F(\mathbf{u}_k) + \mathbb{E}\langle \nabla F(\mathbf{u}_k), -\eta \mathcal{G}_K \rangle + \frac{L}{2} \mathbb{E} \|\eta \mathcal{G}_K\|^2 \\
&= \mathbb{E}F(\mathbf{u}_k) - \eta \mathbb{E} \langle \nabla F(\mathbf{u}_k), \mathcal{Z}_k \rangle + \frac{L\eta^2}{2} \mathbb{E} \|\mathcal{G}_K - \mathcal{Z}_k + \mathcal{Z}_k\|^2 \\
&= \mathbb{E}F(\mathbf{u}_k) - \eta \mathbb{E} \langle \nabla F(\mathbf{u}_k), \mathcal{Z}_k \rangle + \frac{L\eta^2}{2} \mathbb{E} \|\mathcal{G}_K - \mathcal{Z}_k\|^2 + \frac{L\eta^2}{2} \mathbb{E} \|\mathcal{Z}_k\|^2 \\
&\stackrel{(a)}{=} \mathbb{E}F(\mathbf{u}_k) - \eta \sum_{i \in \mathcal{C}} m_i \mathbb{E} \left\langle \nabla F(\mathbf{u}_k), \nabla F_i(\mathbf{w}_k^{(i)}) \right\rangle + \frac{L\eta^2}{2} \mathbb{E} \left\| \sum_{i \in \mathcal{C}} m_i g(\mathbf{w}_k^{(i)}) - m_i \nabla F_i(\mathbf{w}_k^{(i)}) \right\|^2 \\
&\quad + \frac{L\eta^2}{2} \mathbb{E} \|\mathcal{Z}_k\|^2 \\
&\stackrel{(b)}{=} \mathbb{E}F(\mathbf{u}_k) - \eta \sum_{i \in \mathcal{C}} m_i \mathbb{E} \left\langle \nabla F(\mathbf{u}_k), \nabla F_i(\mathbf{w}_k^{(i)}) \right\rangle + \frac{L\eta^2}{2} \sum_{i \in \mathcal{C}} m_i^2 \mathbb{E} \left\| g(\mathbf{w}_k^{(i)}) - \nabla F_i(\mathbf{w}_k^{(i)}) \right\|^2 \\
&\quad + \frac{L\eta^2}{2} \mathbb{E} \|\mathcal{Z}_k\|^2 \\
&\stackrel{(c)}{\leq} \mathbb{E}F(\mathbf{u}_k) - \left(\frac{\eta}{2} \mathbb{E} \|\nabla F(\mathbf{u}_k)\|^2 + \frac{\eta}{2} \sum_{i \in \mathcal{C}} m_i \mathbb{E} \left\| \nabla F_i(\mathbf{w}_k^{(i)}) \right\|^2 - \frac{\eta}{2} \sum_{i \in \mathcal{C}} m_i \mathbb{E} \left\| \nabla F(\mathbf{u}_k) - \nabla F_i(\mathbf{w}_k^{(i)}) \right\|^2 \right) \\
&\quad + \frac{L\eta^2}{2} \sum_{i \in \mathcal{C}} m_i^2 \sigma^2 + \frac{L\eta^2}{2} \mathbb{E} \|\mathcal{Z}_k\|^2 \\
&\stackrel{(d)}{\leq} \mathbb{E}F(\mathbf{u}_k) - \left(\frac{\eta}{2} \mathbb{E} \|\nabla F(\mathbf{u}_k)\|^2 + \frac{\eta}{2} \sum_{i \in \mathcal{C}} m_i \mathbb{E} \left\| \nabla F_i(\mathbf{w}_k^{(i)}) \right\|^2 - \frac{\eta}{2} \sum_{i \in \mathcal{C}} m_i \mathbb{E} \left\| \nabla F(\mathbf{u}_k) - \nabla F_i(\mathbf{w}_k^{(i)}) \right\|^2 \right) \\
&\quad + \frac{L\eta^2}{2} \sum_{i \in \mathcal{C}} m_i^2 \sigma^2 + \frac{LC\eta^2}{2} \sum_{i \in \mathcal{C}} m_i \mathbb{E} \left\| \nabla F_i(\mathbf{w}_k^{(i)}) \right\|^2 \\
&\stackrel{(e)}{=} \mathbb{E}F(\mathbf{u}_k) - \frac{\eta}{2} \mathbb{E} \|\nabla F(\mathbf{u}_k)\|^2 - \left(\frac{\eta}{2} - \frac{LC\eta^2}{2} \right) J_k + \frac{\eta}{2} \sum_{i \in \mathcal{C}} m_i \mathbb{E} \left\| \nabla F(\mathbf{u}_k) - \nabla F_i(\mathbf{w}_k^{(i)}) \right\|^2 + \frac{L\eta^2}{2} \sum_{i \in \mathcal{C}} m_i^2 \sigma^2 \\
&\stackrel{(f)}{\leq} \mathbb{E}F(\mathbf{u}_k) - \frac{\eta}{2} \mathbb{E} \|\nabla F(\mathbf{u}_k)\|^2 - \left(\frac{\eta}{2} - \frac{LC\eta^2}{2} \right) J_k + \frac{\eta L^2}{2} \sum_{i \in \mathcal{C}} m_i \mathbb{E} \left\| \mathbf{u}_k - \mathbf{w}_k^{(i)} \right\|^2 + \frac{L\eta^2}{2} \sum_{i \in \mathcal{C}} m_i^2 \sigma^2 \\
&= \mathbb{E}F(\mathbf{u}_k) - \frac{\eta}{2} \mathbb{E} \|\nabla F(\mathbf{u}_k)\|^2 - \left(\frac{\eta}{2} - \frac{LC\eta^2}{2} \right) J_k + \frac{\eta L^2}{2} \mathbb{E} \|\mathbf{W}_k(\mathbf{I} - \mathbf{M})\|_{\mathbf{M}}^2 + \frac{L\eta^2}{2} \sum_{i \in \mathcal{C}} m_i^2 \sigma^2 \\
&= \mathbb{E}F(\mathbf{u}_k) - \frac{\eta}{2} \mathbb{E} \|\nabla F(\mathbf{u}_k)\|^2 - \frac{\eta}{2} (1 - LC\eta) J_k + \frac{\eta L^2}{2} \mathbb{E} \|\mathbf{W}_k(\mathbf{I} - \mathbf{M})\|_{\mathbf{M}}^2 + \frac{L\eta^2}{2} \sum_{i \in \mathcal{C}} m_i^2 \sigma^2,
\end{aligned} \tag{24}$$

where (a) follows the definition of \mathcal{G}_k and \mathcal{Z}_k . Since $\mathbb{E} \left[g(\mathbf{w}_k^{(i)}) \right] = \nabla F_i(\mathbf{w}_k^{(i)})$, the cross-terms of $\mathbb{E} \left\langle m_i g(\mathbf{w}_k^{(i)}) - m_i \nabla F_i(\mathbf{w}_k^{(i)}), m_j g(\mathbf{w}_k^{(j)}) - m_j \nabla F_j(\mathbf{w}_k^{(j)}) \right\rangle$ are zero and thus (b) holds. (c) follows the assumption of (9), and (d) is due to $\mathbb{E} \|\mathcal{Z}_k\|^2 = \mathbb{E} \left\| \sum_{i \in \mathcal{C}} \sqrt{m_i} (\sqrt{m_i} \nabla F_i(\mathbf{w}_k^{(i)})) \right\|^2 \leq \mathbb{E} \left[\sum_{i \in \mathcal{C}} (\sqrt{m_i})^2 \sum_{i \in \mathcal{C}} (\sqrt{m_i} \nabla F_i(\mathbf{w}_k^{(i)}))^2 \right] \leq C \sum_{i \in \mathcal{C}} m_i \mathbb{E} \left\| \nabla F_i(\mathbf{w}_k^{(i)}) \right\|^2$. We denote $J_k \triangleq \sum_{i \in \mathcal{C}} m_i \mathbb{E} \left\| \nabla F_i(\mathbf{w}_k^{(i)}) \right\|^2$ in (e), and (f) holds because of the L -smoothness assumption of the local loss function in (7). Finally, the proof is completed by moving $\mathbb{E}F(\mathbf{u}_k)$ to the left-hand side of (24). \square

Lemma 6. *The gradient of the global loss function can be bounded as follows:*

$$\mathbb{E} \|\nabla F(\mathbf{W}_k)\|_{\mathbf{M}}^2 \leq \sum_{i \in \mathcal{C}} m_i^2 \kappa^2 + \sum_{i \in \mathcal{C}} m_i \mathbb{E} \left\| \nabla F_i(\mathbf{w}_k^{(i)}) \right\|^2 = \sum_{i \in \mathcal{C}} m_i^2 \kappa^2 + J_k. \tag{25}$$

Proof. The proof can be obtained by applying the definition of non-IIDness in (10) as follows:

$$\mathbb{E} \|\nabla F(\mathbf{W}_k)\|_{\mathbf{M}}^2 \leq \mathbb{E} \|\nabla F(\mathbf{W}_k) - \mathbf{Z}_k + \mathbf{Z}_k\|_{\mathbf{M}}^2$$

$$\begin{aligned}
&= \mathbb{E} \|\nabla F(\mathbf{W}_k) - \mathbf{Z}_k\|_{\mathbf{M}}^2 + \mathbb{E} \|\mathbf{Z}_k\|_{\mathbf{M}}^2 \\
&\leq \sum_{i \in \mathcal{C}} m_i^2 \mathbb{E} \left\| \nabla F(\mathbf{w}_k^{(i)}) - \nabla F_i(\mathbf{w}_k^{(i)}) \right\|^2 + \mathbb{E} \|\mathbf{Z}_k\|_{\mathbf{M}}^2 \\
&\leq \sum_{i \in \mathcal{C}} m_i^2 \kappa^2 + \sum_{i \in \mathcal{C}} m_i \mathbb{E} \left\| \nabla F_i(\mathbf{w}_k^{(i)}) \right\|^2.
\end{aligned} \tag{26}$$

□

Lemma 7. \mathbf{H}_1 and \mathbf{H}_2 have the following properties:

$$\|\mathbf{H}_1 - \mathbf{M}\|_{\text{op}} = 1, \tag{27}$$

$$\|\mathbf{H}_2^j - \mathbf{M}\|_{\text{op}} = \zeta^{j\alpha}, \tag{28}$$

where $\|\cdot\|_{\text{op}} \triangleq \max_{\|\mathbf{w}\|=1} \mathbf{X}\mathbf{w} = \sqrt{\lambda_{\max}(\mathbf{X}^T \mathbf{X})}$ denotes the operator norm.

Proof. According to Lemma 3 and the definition of the matrix operation norm, we have:

$$\|\mathbf{H}_2^j - \mathbf{M}\|_{\text{op}} = \sqrt{\lambda_{\max}((\mathbf{H}_2^j - \mathbf{M})^T(\mathbf{H}_2^j - \mathbf{M}))} = \sqrt{\lambda_{\max}(\mathbf{H}_2^{2j} - \mathbf{M}^2)} = \sqrt{\lambda_{\max}(\mathbf{H}_2 - \mathbf{M})^{2j}} = \zeta^{j\alpha}. \tag{29}$$

In particular, by plugging $\alpha = 0$ in (29), we have $\|\mathbf{H}_1 - \mathbf{M}\|_{\text{op}} = \zeta^{j0} = 1$. □

Lemma 8. Denote $T_1(j, l, f) \triangleq 2\eta^2 \mathbb{E} \left[\left\| \sum_{r=0}^{j-1} (Y_r - Q_r)(\mathbf{H}_1^{j-r} - \mathbf{M}) + (Y_{j,l}^{(1)} - Q_{j,l}^{(1)}) (\mathbf{H}_2 - \mathbf{M}) + (Y_{j,l,f}^{(2)} - Q_{j,l,f}^{(2)}) (\mathbf{I} - \mathbf{M}) \right\|_{\mathbf{M}}^2 \right]$.

Summing $T_1(j, l, f)$ over all iterations yields an upper bound as follows:

$$\sum_{j=0}^{K/(\tau_1\tau_2)-1} \sum_{l=0}^{\tau_2-1} \sum_{f=1}^{\tau_1} T_1 \leq 2\eta^2 K \sum_{i \in \mathcal{C}} m_i^2 \left[\tau_1^2 \tau_2^2 \Lambda + \frac{2 - \zeta^\alpha}{1 - \zeta^\alpha} \left(\tau_1^2 \frac{(\tau_2 - 1)(2\tau_2 + 1)}{6} + \frac{(\tau_1 - 1)(2\tau_1 + 1)}{6} \right) \right] (\sigma^2 + \kappa^2), \tag{30}$$

where $\Lambda = \left(\frac{\zeta^{2\alpha}}{1 - \zeta^{2\alpha}} + \frac{2\zeta^\alpha}{1 - \zeta^\alpha} + \frac{\zeta^{2\alpha}}{(1 - \zeta^\alpha)^2} \right)$.

Proof. According to the definition of $T_1(j, l, f)$, we have

$$\begin{aligned}
T_1(j, l, f) &= 2\eta^2 \left(\sum_{r=0}^{j-1} \mathbb{E} \left\| (Y_r - Q_r)(\mathbf{H}_1^{j-r} - \mathbf{M}) \right\|_{\mathbf{M}}^2 + \mathbb{E} \left\| (Y_{v,l}^{(1)} - Q_{v,l}^{(1)}) (\mathbf{H}_2 - \mathbf{M}) \right\|_{\mathbf{M}}^2 + \mathbb{E} \left\| (Y_{v,l,f}^{(2)} - Q_{v,l,f}^{(2)}) (\mathbf{I} - \mathbf{M}) \right\|_{\mathbf{M}}^2 \right) \\
&\quad + 2\eta^2 \underbrace{\sum_{n=0}^{j-1} \sum_{l=0, l \neq n}^{j-1} \mathbb{E} \left[\underbrace{\text{Tr} \left((\mathbf{H}_1^{j-n} - \mathbf{M})(Y_n - Q_n)^T (Y_l - Q_l)(\mathbf{H}_1^{j-l} - \mathbf{M}) \right)}_{\text{Trace-1}} \right]}_{\text{Term-1}} \\
&\quad + 4\eta^2 \underbrace{\sum_{l=0}^{j-1} \mathbb{E} \left[\text{Tr} \left((\mathbf{H}_2 - \mathbf{M})(Y_{v,l}^{(1)} - Q_{v,l}^{(1)})^T (Y_l - Q_l)(\mathbf{H}_1^{j-l} - \mathbf{M}) \right) \right]}_{\text{Term-2}} \\
&\quad + 4\eta^2 \underbrace{\sum_{l=0}^{j-1} \mathbb{E} \left[\text{Tr} \left((\mathbf{I} - \mathbf{M})(Y_{v,l,f}^{(2)} - Q_{v,l,f}^{(2)})^T (Y_l - Q_l)(\mathbf{H}_1^{j-l} - \mathbf{M}) \right) \right]}_{\text{Term-3}} \\
&\quad + 4\eta^2 \underbrace{\sum_{l=0}^{j-1} \mathbb{E} \left[\text{Tr} \left((\mathbf{H}_2 - \mathbf{M})(Y_{v,l}^{(1)} - Q_{v,l}^{(1)})^T (Y_{v,l,f}^{(2)} - Q_{v,l,f}^{(2)}) (\mathbf{I} - \mathbf{M}) \right) \right]}_{\text{Term-4}},
\end{aligned} \tag{31}$$

□

where the four traces in Terms 1-4 can be bounded similarly and thus we only bound the first trace, namely Trace-1, as follows:

$$\begin{aligned}
\text{Trace-1} &\leq \left\| (\mathbf{H}_1^{j-n} - \mathbf{M})(Y_n - Q_n) \right\|_{\mathbf{M}} \left\| (Y_l - Q_l)(\mathbf{H}_1^{j-l} - \mathbf{M}) \right\|_{\mathbf{M}} \\
&\leq \left\| \mathbf{H}_1^{j-n} - \mathbf{M} \right\|_{\text{op}} \|Y_n - Q_n\|_{\mathbf{M}} \|Y_l - Q_l\|_{\mathbf{M}} \left\| \mathbf{H}_1^{j-l} - \mathbf{M} \right\|_{\text{op}} \\
&\leq \zeta^{(2j-n-l)\alpha} \|Y_n - Q_n\|_{\mathbf{M}} \|Y_l - Q_l\|_{\mathbf{M}} \\
&\leq \frac{1}{2} \zeta^{(2j-n-l)\alpha} \left[\|Y_n - Q_n\|_{\mathbf{M}}^2 + \|Y_l - Q_l\|_{\mathbf{M}}^2 \right].
\end{aligned} \tag{32}$$

As a result, the RHS of (31) is bounded as follows:

$$\begin{aligned}
&\text{Term-1} + \text{Term-2} + \text{Term-3} + \text{Term-4} \\
&\leq \eta^2 \sum_{n=0}^{j-1} \sum_{l=0, l \neq n}^{j-1} \zeta^{(2j-n-l)\alpha} \left[\mathbb{E} \|Y_n - Q_n\|_{\mathbf{M}}^2 + \mathbb{E} \|Y_l - Q_l\|_{\mathbf{M}}^2 \right] + 2\eta^2 \sum_{l=0}^{j-1} \zeta^{(j-l)\alpha} \left[\mathbb{E} \left\| Y_{v,l}^{(1)} - Q_{v,l}^{(1)} \right\|_{\mathbf{M}}^2 + \mathbb{E} \|Y_l - Q_l\|_{\mathbf{M}}^2 \right] \\
&\quad + 2\eta^2 \sum_{l=0}^{j-1} \zeta^{(j-l)\alpha} \left[\mathbb{E} \left\| Y_{v,l,f}^{(2)} - Q_{v,l,f}^{(2)} \right\|_{\mathbf{M}}^2 + \mathbb{E} \|Y_l - Q_l\|_{\mathbf{M}}^2 \right] + 2\eta^2 \sum_{l=0}^{j-1} \zeta^{(j-l)\alpha} \left[\mathbb{E} \left\| Y_{v,l}^{(1)} - Q_{v,l}^{(1)} \right\|_{\mathbf{M}}^2 + \mathbb{E} \left\| Y_{v,l,f}^{(2)} - Q_{v,l,f}^{(2)} \right\|_{\mathbf{M}}^2 \right] \\
&\leq 2\eta^2 \sum_{n=0}^{j-1} \zeta^{(j-n)\alpha} \mathbb{E} \|Y_n - Q_n\|_{\mathbf{M}}^2 \sum_{l=0, l \neq n}^{j-1} \zeta^{(j-l)\alpha} + 4\eta^2 \sum_{l=0}^{j-1} \zeta^{(j-l)\alpha} \mathbb{E} \|Y_l - Q_l\|_{\mathbf{M}}^2 \\
&\quad + 2\eta^2 \mathbb{E} \left\| Y_{v,l}^{(1)} - Q_{v,l}^{(1)} \right\|_{\mathbf{M}}^2 \sum_{l=0}^j \zeta^{(j-l)\alpha} + 2\eta^2 \mathbb{E} \left\| Y_{v,l,f}^{(2)} - Q_{v,l,f}^{(2)} \right\|_{\mathbf{M}}^2 \sum_{l=0}^j \zeta^{(j-l)\alpha}.
\end{aligned} \tag{33}$$

We further observe that

$$\mathbb{E} \left\| Y_{j,l}^{(1)} - Q_{j,l}^{(1)} \right\|_{\mathbf{M}}^2 \leq l^2 \tau_1^2 \sum_{i \in \mathcal{C}} m_i^2 (\sigma^2 + \kappa^2), \tag{34}$$

$$\mathbb{E} \left\| Y_{j,l,f}^{(2)} - Q_{j,l,f}^{(2)} \right\|_{\mathbf{M}}^2 \leq (f-1)^2 \sum_{i \in \mathcal{C}} m_i^2 (\sigma^2 + \kappa^2), \tag{35}$$

$$\mathbb{E} \|Y_r - Q_r\|_{\mathbf{M}}^2 \leq \tau_1^2 \tau_2^2 \sum_{i \in \mathcal{C}} m_i^2 (\sigma^2 + \kappa^2). \tag{36}$$

By defining $\Lambda_{j-r} \triangleq \zeta^{2(j-r)\alpha} + 2\zeta^{(j-r)\alpha} + \frac{\zeta^{(j-r+1)\alpha}}{1-\zeta^\alpha}$, we have

$$\sum_{j=0}^{K/\tau_1\tau_2-1} \sum_{r=0}^{j-1} \Lambda_{j-r} \leq \left(\frac{K}{\tau_1\tau_2} - 1 \right) \Lambda, \tag{37}$$

where $\Lambda \triangleq \frac{\zeta^{2\alpha}}{1-\zeta^{2\alpha}} + \frac{2\zeta^\alpha}{1-\zeta^\alpha} + \frac{\zeta^{2\alpha}}{(1-\zeta^\alpha)^2}$. Thus, $T_1(j, l, f)$ can be bounded as follows:

$$T_1(j, l, f) \leq 2\eta^2 \sum_{r=0}^{j-1} \Lambda_{j-r} \tau_1^2 \tau_2^2 \sum_{i \in \mathcal{C}} m_i^2 (\sigma^2 + \kappa^2) + 2\eta^2 \frac{2-\zeta^\alpha}{1-\zeta^\alpha} l^2 \tau_1^2 \sum_{i \in \mathcal{C}} m_i^2 (\sigma^2 + \kappa^2) + 2\eta^2 \frac{2-\zeta^\alpha}{1-\zeta^\alpha} (f-1)^2 \sum_{i \in \mathcal{C}} m_i^2 (\sigma^2 + \kappa^2). \tag{38}$$

We sum up $T_1(j, l, f)$ over $f = 1, \dots, \tau_1$ and $l = 0, \dots, \tau_2 - 1$, yielding the following results:

$$\sum_{l=0}^{\tau_2-1} \sum_{f=1}^{\tau_1} T_1(j, l, f) \leq 2\eta^2 \sum_{i \in \mathcal{C}} m_i^2 \left[\tau_1^3 \tau_2^3 \Lambda_{j-r} + \frac{2-\zeta^\alpha}{1-\zeta^\alpha} \left(\tau_1^3 \frac{\tau_2(\tau_2-1)(2\tau_2+1)}{6} + \tau_2 \frac{\tau_1(\tau_1-1)(2\tau_1+1)}{6} \right) \right] (\sigma^2 + \kappa^2). \tag{39}$$

Finally, by summing up both sides of (39) over $j = 0, 1, \dots, K/(\tau_1\tau_2) - 1$, we have:

$$\sum_{j=0}^{K/(\tau_1\tau_2)-1} \sum_{l=0}^{\tau_2-1} \sum_{f=1}^{\tau_1} T_1(j, l, f)$$

$$\begin{aligned}
&\stackrel{(a)}{\leq} 2\eta^2 \sum_{i \in \mathcal{C}} m_i^2 \left[\tau_1^3 \tau_2^3 \left(\frac{K}{\tau_1 \tau_2} - 1 \right) \Lambda + K \frac{2 - \zeta^\alpha}{1 - \zeta^\alpha} \left(\tau_1^2 \frac{(\tau_2 - 1)(2\tau_2 + 1)}{6} + \frac{(\tau_1 - 1)(2\tau_1 + 1)}{6} \right) \right] (\sigma^2 + \kappa^2) \\
&\leq 2\eta^2 K \sum_{i \in \mathcal{C}} m_i^2 \left[\tau_1^2 \tau_2^2 \Lambda + \frac{2 - \zeta^\alpha}{1 - \zeta^\alpha} \left(\tau_1^2 \frac{(\tau_2 - 1)(2\tau_2 + 1)}{6} + \frac{(\tau_1 - 1)(2\tau_1 + 1)}{6} \right) \right] (\sigma^2 + \kappa^2),
\end{aligned} \tag{40}$$

where (a) holds because of (37). \square

Lemma 9. Denote $T_2(j, l, f) \triangleq 2\eta^2 \mathbb{E} \left[\left\| \sum_{r=0}^{j-1} Q_r (\mathbf{H}_1^{j-r} - \mathbf{M}) + Q_{j,l}^{(1)} (\mathbf{H}_2 - \mathbf{M}) + Q_{j,l,f}^{(2)} (\mathbf{I} - \mathbf{M}) \right\|_{\mathbf{M}}^2 \right]$. Summing $T_2(j, l, f)$ over $k = 1, 2, \dots, K$ yields an upper bound as follows:

$$\sum_{j=0}^{K/(\tau_1 \tau_2)-1} \sum_{l=0}^{\tau_2-1} \sum_{f=1}^{\tau_1} T_2(j, l, f) \leq 2\eta^2 \tau_1^2 \tau_2^2 \left(\Lambda + \frac{2(\tau_1 - 1)}{\tau_1} \right) \sum_{k=1}^K \left(\sum_{i \in \mathcal{C}} m_i^2 \kappa^2 + J_k \right). \tag{41}$$

Proof. According to the definition of $T_2(j, l, f)$, we have:

$$\begin{aligned}
T_2(j, l, f) &\leq 2\eta^2 \sum_{r=0}^{j-1} \left(\zeta^{2(j-r)\alpha} + 2\zeta^{(j-r)\alpha} + \frac{\zeta^{(j-r+1)\alpha}}{1 - \zeta^\alpha} \right) \mathbb{E} \|Q_r\|_{\mathbf{M}}^2 \\
&\quad + 2\eta^2 \left(\frac{2 - \zeta^\alpha}{1 - \zeta^\alpha} \right) \mathbb{E} \|Q_{j,l}^{(1)}\|_{\mathbf{M}}^2 + 2\eta^2 \left(\frac{2 - \zeta^\alpha}{1 - \zeta^\alpha} \right) \mathbb{E} \|Q_{j,l,f}^{(2)}\|_{\mathbf{M}}^2 \\
&\stackrel{(a)}{=} 2\eta^2 \sum_{r=0}^{j-1} \Lambda_{j-r} \mathbb{E} \left\| \sum_{s=1}^{\tau_1 \tau_2} \nabla F(X_{r\tau_1 \tau_2+s}) \right\|_{\mathbf{M}}^2 \\
&\quad + 2\eta^2 \left(\frac{2 - \zeta^\alpha}{1 - \zeta^\alpha} \right) \mathbb{E} \left\| \sum_{s=1}^{l\tau_1} \nabla F(X_{j\tau_1 \tau_2+s}) \right\|_{\mathbf{M}}^2 + 2\eta^2 \left(\frac{2 - \zeta^\alpha}{1 - \zeta^\alpha} \right) \mathbb{E} \left\| \sum_{s=1}^{f-1} \nabla F(X_{j\tau_1 \tau_2+l\tau_1+s}) \right\|_{\mathbf{M}}^2 \\
&\leq 2\eta^2 \tau_1 \tau_2 \sum_{r=0}^{j-1} \Lambda_{j-r} \sum_{s=1}^{\tau_1 \tau_2} \mathbb{E} \|\nabla F(X_{r\tau_1 \tau_2+s})\|_{\mathbf{M}}^2 \\
&\quad + 2\eta^2 l \tau_1 \left(\frac{2 - \zeta^\alpha}{1 - \zeta^\alpha} \right) \sum_{s=1}^{l\tau_1} \mathbb{E} \|\nabla F(X_{j\tau_1 \tau_2+s})\|_{\mathbf{M}}^2 + 2\eta^2 (f-1) \left(\frac{2 - \zeta^\alpha}{1 - \zeta^\alpha} \right) \sum_{s=1}^{f-1} \mathbb{E} \|\nabla F(X_{j\tau_1 \tau_2+l\tau_1+s})\|_{\mathbf{M}}^2,
\end{aligned} \tag{42}$$

where (a) holds due to the following inequalities:

$$\mathbb{E} \|Q_{j,l}^{(1)}\|_{\mathbf{M}}^2 \leq \tau_1 \tau_2 \sum_{s=1}^{\tau_1 \tau_2} \mathbb{E} \|\nabla F(\mathbf{W}_{r\tau_1 \tau_2+s})\|_{\mathbf{M}}^2, \tag{43}$$

$$\mathbb{E} \|Q_{j,l,f}^{(2)}\|_{\mathbf{M}}^2 \leq l \tau_1 \sum_{s=1}^{l\tau_1} \mathbb{E} \|\nabla F(\mathbf{W}_{j\tau_1 \tau_2+s})\|_{\mathbf{M}}^2, \tag{44}$$

$$\mathbb{E} \|Q_r\|_{\mathbf{M}}^2 \leq (f-1) \sum_{s=1}^{f-1} \mathbb{E} \|\nabla F(\mathbf{W}_{j\tau_1 \tau_2+l\tau_1+s})\|_{\mathbf{M}}^2. \tag{45}$$

By summing $T_2(j, l, f)$ over $f = 1, \dots, \tau_1$ and $l = 0, \dots, \tau_2 - 1$, we obtain:

$$\begin{aligned}
\sum_{l=0}^{\tau_2-1} \sum_{f=1}^{\tau_1} T_2(j, l, f) &\leq 2\eta^2 \tau_1^2 \tau_2^2 \sum_{i=1}^{j-1} \Lambda_{j-r} \sum_{s=1}^{\tau_1 \tau_2} \mathbb{E} \|\nabla F(X_{r\tau_1 \tau_2+s})\|_{\mathbf{M}}^2 \\
&\quad + 2\eta^2 \left(\frac{2 - \zeta^\alpha}{1 - \zeta^\alpha} \right) \sum_{l=0}^{\tau_2-1} \sum_{f=1}^{\tau_1} \left(l \tau_1 \sum_{s=1}^{l\tau_1} \mathbb{E} \|\nabla F(X_{j\tau_1 \tau_2+s})\|_{\mathbf{M}}^2 + (f-1) \sum_{s=1}^{f-1} \mathbb{E} \|\nabla F(X_{j\tau_1 \tau_2+l\tau_1+s})\|_{\mathbf{M}}^2 \right).
\end{aligned} \tag{46}$$

Notice that for any function $\beta(s)$, we have:

$$\sum_{j=0}^{K/(\tau_1 \tau_2)-1} \sum_{l=0}^{\tau_2-1} \sum_{f=1}^{\tau_1} \left(l \tau_1 \sum_{s=j\tau_2 \tau_1}^{j\tau_2 \tau_1 + l\tau_1} \beta(s) + (f-1) \sum_{s=j\tau_2 \tau_1 + l\tau_1 + 1}^{j\tau_2 \tau_1 + l\tau_1 + f-1} \beta(s) \right) \leq \left(\frac{\tau_2(\tau_2 - 1)}{2} \tau_1^2 + \frac{\tau_1(\tau_1 - 1)}{2} \tau_2 \right) \sum_{k=1}^K \beta(k). \tag{47}$$

By further summing both sides of (46) over $j = 0, 1, \dots, K/(\tau_1\tau_2) - 1$ and applying (47), we have:

$$\begin{aligned}
& \sum_{j=0}^{K/(\tau_1\tau_2)-1} \sum_{l=0}^{\tau_2-1} \sum_{f=1}^{\tau_1} T_2(j, l, f) \\
& \leq 2\eta^2 \tau_1^2 \tau_2^2 \Lambda \sum_{j=1}^{K/\tau_1\tau_2-1} \sum_{s=1}^{\tau_1\tau_2} \mathbb{E} \|\nabla F(X_{r\tau_1\tau_2+s})\|_{\mathbf{M}}^2 + 2\eta^2 \left(\frac{\tau_2(\tau_2-1)}{2} \tau_1^2 + \frac{\tau_1(\tau_1-1)}{2} \tau_2 \right) \sum_{k=1}^K \mathbb{E} \|\nabla F(X_k)\|_{\mathbf{M}}^2 \\
& \stackrel{(a)}{\leq} 2\eta^2 \tau_1^2 \tau_2^2 \Lambda \sum_{k=1}^K \mathbb{E} \|\nabla F(X_k)\|_{\mathbf{M}}^2 + 2\eta^2 \left(\frac{\tau_2(\tau_2-1)}{2} \tau_1^2 + \frac{\tau_1(\tau_1-1)}{2} \tau_2 \right) \sum_{k=1}^K \mathbb{E} \|\nabla F(X_k)\|_{\mathbf{M}}^2 \\
& = 2\eta^2 \tau_1^2 \tau_2^2 \left(\frac{\zeta^{2\alpha}}{1-\zeta^{2\alpha}} + \frac{2\zeta}{1-\zeta} + \frac{\zeta^{2\alpha}}{(1-\zeta)^2} + \frac{2(\tau_1-1)}{\tau_1} \right) \sum_{k=1}^K \mathbb{E} \|\nabla F(X_k)\|_{\mathbf{M}}^2 \\
& \stackrel{(b)}{\leq} 2\eta^2 \tau_1^2 \tau_2^2 \left(\frac{\zeta^{2\alpha}}{1-\zeta^{2\alpha}} + \frac{2\zeta}{1-\zeta} + \frac{\zeta^{2\alpha}}{(1-\zeta)^2} + \frac{2(\tau_1-1)}{\tau_1} \right) \sum_{k=1}^K \left[\sum_{i \in \mathcal{C}} m_i^2 \kappa^2 + \sum_{i \in \mathcal{C}} m_i \mathbb{E} \|\nabla F_i(\mathbf{w}_k^{(i)})\|^2 \right] \\
& = 2\eta^2 \tau_1^2 \tau_2^2 \left(\Lambda + \frac{2(\tau_1-1)}{\tau_1} \right) \sum_{k=1}^K \left[\sum_{i \in \mathcal{C}} m_i^2 \kappa^2 + \sum_{i \in \mathcal{C}} m_i \mathbb{E} \|\nabla F_i(\mathbf{w}_k^{(i)})\|^2 \right] \\
& = 2\eta^2 \tau_1^2 \tau_2^2 \left(\Lambda + \frac{2(\tau_1-1)}{\tau_1} \right) \sum_{k=1}^K \left(\sum_{i \in \mathcal{C}} m_i^2 \kappa^2 + J_k \right),
\end{aligned} \tag{48}$$

where (a) follows (47) and (b) uses the results derived in Lemma 6. \square

C. Proof of Lemma 2

First, we rewrite $\mathbf{W}_k(\mathbf{I} - \mathbf{M})$ as follows:

$$\begin{aligned}
& \mathbf{W}_k(\mathbf{I} - \mathbf{M}) \\
& \stackrel{(a)}{=} ((\mathbf{W}_{k-1} - \eta \mathbf{G}_{k-1}) \mathbf{T}_{k-1}(\mathbf{I} - \mathbf{M})) \\
& \stackrel{(b)}{=} \mathbf{W}_{k-1}(\mathbf{I} - \mathbf{M}) \mathbf{T}_{k-1} - \eta \mathbf{G}_{k-1}(\mathbf{T}_{k-1} - \mathbf{M}) \\
& \stackrel{(c)}{=} [(\mathbf{W}_{k-2} - \eta \mathbf{G}_{k-2}) \mathbf{T}_{k-2}(\mathbf{I} - \mathbf{M})] \mathbf{T}_{k-1} - \eta \mathbf{G}_{k-1}(\mathbf{T}_{k-1} - \mathbf{M}) \\
& \stackrel{(d)}{=} \mathbf{W}_{k-2}(\mathbf{I} - \mathbf{M}) \mathbf{T}_{k-2} \mathbf{T}_{k-1} - \eta \mathbf{G}_{k-2}(\mathbf{T}_{k-2} \mathbf{T}_{k-1} - \mathbf{M}) \eta \mathbf{G}_{k-1}(\mathbf{T}_{k-1} - \mathbf{M}),
\end{aligned} \tag{49}$$

where (a) and (c) follow (11), while (b) and (d) follow Lemma 4. By mathematical induction, we obtain:

$$\begin{aligned}
& \mathbf{W}_k(\mathbf{I} - \mathbf{M}) \\
& = \mathbf{W}_0(\mathbf{I} - \mathbf{M}) \prod_{l=0}^{k-1} \mathbf{T}_l - \eta \sum_{s=0}^{k-1} \mathbf{G}_s \left(\prod_{l=s}^{k-1} \mathbf{T}_l - \mathbf{M} \right) \\
& \stackrel{(e)}{=} \eta \sum_{s=0}^{k-1} \mathbf{G}_s \left(\prod_{l=s}^{k-1} \mathbf{T}_l - \mathbf{M} \right),
\end{aligned} \tag{50}$$

where (e) holds since $\mathbf{W}_0 = [\mathbf{w}_0, \dots, \mathbf{w}_0]$, i.e., $\mathbf{W}_0(\mathbf{I} - \mathbf{M}) = 0$.

Denote $\Phi_{s,k-1} \triangleq \prod_{l=s}^{k-1} \mathbf{T}_l$, which can be expressed as:

$$\Phi_{s,k-1} = \begin{cases} \mathbf{I}, & \text{if } j\tau_2\tau_1 + l\tau_1 < s < j\tau_2\tau_1 + l\tau_1 + f, \\ \mathbf{H}_1, & \text{if } j\tau_2\tau_1 < s \leq j\tau_2\tau_1 + l\tau_1, \\ \mathbf{H}_2, & \text{if } (j-1)\tau_2\tau_1 + l\tau_1 < s \leq j\tau_2\tau_1, \\ \dots \\ \mathbf{H}_2^j, & \text{if } 1 \leq s \leq \tau_2\tau_1. \end{cases} \tag{51}$$

With the results in (50) and (51), we derive an upper bound for $\mathbb{E} [\|\mathbf{W}_k(\mathbf{I} - \mathbf{M})\|_{\mathbf{M}}^2]$ as follows:

$$\begin{aligned}
& \mathbb{E} \left[\|\mathbf{W}_k(\mathbf{I} - \mathbf{M})\|_{\mathbf{M}}^2 \right] \\
&= \eta^2 \mathbb{E} \left[\left\| \sum_{r=0}^{j-1} Y_r(\mathbf{H}_1^{j-r} - \mathbf{M}) + Y_{j,l}^{(1)}(\mathbf{H}_2 - \mathbf{M}) + Y_{j,l,f}^{(2)}(\mathbf{I} - \mathbf{M}) \right\|_{\mathbf{M}}^2 \right] \\
&\leq 2\eta^2 \mathbb{E} \underbrace{\left[\left\| \sum_{r=0}^{j-1} (Y_r - Q_r)(\mathbf{H}_1^{j-r} - \mathbf{M}) + (Y_{j,l}^{(1)} - Q_{j,l}^{(1)})(\mathbf{H}_2 - \mathbf{M}) + (Y_{j,l,f}^{(2)} - Q_{j,l,f}^{(2)})(\mathbf{I} - \mathbf{M}) \right\|_{\mathbf{M}}^2 \right]}_{T_1(j,l,f)} \\
&\quad + 2\eta^2 \mathbb{E} \underbrace{\left[\left\| \sum_{r=0}^{j-1} Q_r(\mathbf{H}_1^{j-r} - \mathbf{M}) + Q_{j,l}^{(1)}(\mathbf{H}_2 - \mathbf{M}) + Q_{j,l,f}^{(2)}(\mathbf{I} - \mathbf{M}) \right\|_{\mathbf{M}}^2 \right]}_{T_2(j,l,f)}. \tag{52}
\end{aligned}$$

We complete the proof by summing both sides of (52) over all iterations and further applying the bounds of $T_1(j,l,f)$ and $T_2(j,l,f)$ derived in Lemma 8 and Lemma 9 respectively, \square

D. Proof of Theorem 1

First, we sum up (22) in Lemma 5 for $k = 1, \dots, K$, and divide both sides by K as follows:

$$\begin{aligned}
\frac{1}{K} (\mathbb{E}F(\mathbf{u}_{K+1}) - \mathbb{E}F(\mathbf{u}_1)) &\leq -\frac{\eta}{2K} \sum_{k=1}^K \mathbb{E} \|\nabla F(\mathbf{u}_k)\|^2 + \frac{L\eta^2}{2} \sum_{i \in \mathcal{C}} m_i^2 \sigma^2 \\
&\quad + \frac{\eta L^2}{2} \frac{1}{K} \sum_{k=1}^K \mathbb{E} \|\mathbf{W}_k(\mathbf{I} - \mathbf{M})\|_{\mathbf{M}}^2 - \frac{\eta}{2} (1 - LC\eta) \frac{1}{K} \sum_{k=1}^K J_k. \tag{53}
\end{aligned}$$

By rearranging terms, multiplying each of them by $\frac{2}{\eta}$, we arrive at the following expression:

$$\begin{aligned}
& \frac{1}{K} \sum_{k=1}^K \mathbb{E} \|\nabla F(\mathbf{u}_k)\|^2 \\
&\stackrel{(a)}{\leq} \frac{2[\mathbb{E}F(\mathbf{u}_{K+1}) - \mathbb{E}F(\mathbf{u}_1)]}{\eta K} + L\eta \sum_{i \in \mathcal{C}} m_i^2 \sigma^2 - (1 - LC\eta) \frac{1}{K} \sum_{k=1}^K J_k \\
&\quad + L^2 \times \left\{ 2\eta^2 \sum_{i \in \mathcal{C}} m_i \left[\tau_1^2 \tau_2^2 \Lambda + \frac{2 - \zeta^\alpha}{1 - \zeta^\alpha} \left(\frac{\tau_2(\tau_2 - 1)(2\tau_2 + 1)}{6} + \frac{(\tau_1 - 1)(2\tau_1 + 1)}{6} \right) \right] \right. \\
&\quad \left. (\sigma^2 + \kappa^2) + 2\eta^2 \tau_1^2 \tau_2^2 \sum_{i \in \mathcal{C}} m_i^2 \left(\Lambda + \frac{2(\tau_1 - 1)}{\tau_1} \right) \kappa^2 + 2\eta^2 \tau_1^2 \tau_2^2 \left(\Lambda + \frac{2(\tau_1 - 1)}{\tau_1} \right) \frac{1}{K} \sum_{k=1}^K J_k \right\} \\
&= \frac{2\Delta}{\eta K} + L\eta \sum_{i \in \mathcal{C}} m_i^2 \sigma^2 + 2L^2 \eta^2 V_1 (\sigma^2 + \kappa^2) + 2L^2 \eta^2 V_2 \sum_{i \in \mathcal{C}} m_i^2 \kappa^2 - (1 - LC\eta - 2L^2 \eta^2 V_2) \frac{1}{K} \sum_{k=1}^K J_k,
\end{aligned} \tag{54}$$

where (a) holds jointly attributed to Lemma 2, the Jensen's Inequality, and $\Delta \triangleq \mathbb{E}[F(\mathbf{u}_1)] - \mathbb{E}[F(\mathbf{u}^*)] \geq \mathbb{E}[F(\mathbf{u}_1)] - \mathbb{E}[F(\mathbf{u}_{K+1})]$. As a result, if η satisfies

$$1 - LC\eta - 2L^2 \eta^2 V_2 \geq 0, \tag{55}$$

we have:

$$\frac{1}{K} \sum_{k=1}^K \mathbb{E} \|\nabla F(\mathbf{u}_k)\|^2 \leq \frac{2\Delta}{\eta K} + L\eta \sum_{i \in \mathcal{C}} m_i^2 \sigma^2 + 2L^2 \eta^2 V_1 \sigma^2 + 2L^2 \eta^2 (V_1 + V_2 \sum_{i \in \mathcal{C}} m_i^2) \kappa^2, \tag{56}$$

which completes the proof. \square

E. Proof of Corollary 1

By substituting $\eta = \frac{1}{L} \sqrt{\frac{1}{K \sum_{i \in \mathcal{C}} m_i^2}}$ into the RHS of (16), we have:

$$\begin{aligned} \frac{1}{K} \sum_{k=1}^K \mathbb{E} \|\nabla F(\mathbf{u}_k)\|^2 &\leq \frac{2L\Delta \sqrt{K \sum_{i \in \mathcal{C}} m_i^2}}{K} + \frac{\sum_{i \in \mathcal{C}} m_i^2}{\sqrt{K \sum_{i \in \mathcal{C}} m_i^2}} \sigma^2 + \frac{2V_1}{K \sum_{i \in \mathcal{C}} m_i^2} \sigma^2 + \left(\frac{2V_1}{K \sum_{i \in \mathcal{C}} m_i^2} + \frac{2V_2}{K} \right) \kappa^2 \\ &= \frac{(2L\Delta + \sigma^2) \sqrt{\sum_{i \in \mathcal{C}} m_i^2}}{\sqrt{K}} + \frac{\frac{2V_1}{\sum_{i \in \mathcal{C}} m_i^2} \sigma^2 + \left(\frac{2V_1}{\sum_{i \in \mathcal{C}} m_i^2} + 2V_2 \right) \kappa^2}{K}. \end{aligned} \quad (57)$$

If K is sufficiently large, the first term dominates the RHS of the last inequality (57). In other words, it takes $\mathcal{O}(\frac{1}{\epsilon^2})$ iterations to obtain an ϵ -accurate solution, i.e., $\frac{1}{K} \sum_{k=1}^K \mathbb{E} \|\nabla F(\mathbf{u}_k)\|^2 \leq \epsilon$. \square